Journal of Mechatronics, Electrical Power, and Vehicular Technology 14 (2023) 114-126

Journal of Mechatronics, Electrical Power, and Vehicular Technology

e-ISSN: 2088-6985
p-ISSN: 2087-3379

mev.brin.go.id

An open-source parallel gripper with an embedded soft skin fingertip sensor

Muhammad Arifin [a, *], Rian Putra Pratama [a], Oka Mahendra [a], Aris Munandar [a], Catur Hilman Adritya Haryo Bhakti Baskoro [a], Muhtadin [b, *], Abdullah Iskandar [c]

[a] *Research Center for Smart Mechatronics, National Research and Innovation Agency*
Kawasan Sains dan Teknologi (KST) Samaun Samadikun, Jl. Sangkuriang, Bandung, 40135, Indonesia
[b] *Department of Computer Engineering, Institut Teknologi Sepuluh Nopember*
Kampus ITS Sukolilo, Surabaya, 60111, Indonesia
[c] *Department of Computer Science and Communications Engineering, Waseda University*
3 Chome-4-1 Okubo, Shinjuku City, Tokyo, 169-8555, Japan

Received 13 November 2023; 1st revision 11 December 2023; 2nd revision 16 December 2023;
Accepted 18 December 2023; Published online 29 December 2023

Abstract

The demand for implementing robots into our daily lives has surged in recent years, necessitating safe grasping for effective interaction with the environment. However, a majority of researchers rely on commercial grippers for their experimental studies, which are typically expensive and not accessible to everyone. Despite the existence of open-source designs, the assembly process is often challenging and requires modifications to enhance secure grasping. This paper presents a simple, compact, and low-cost gripper to offer an accessible and readily deployable solution for research and education. The gripper utilizes a parallel four-bar linkage mechanism, minimizing the number of components and incorporating off-the-shelf parts for straightforward assembly. Furthermore, to enhance its capabilities, the proposed gripper implements a soft skin tactile sensor on its fingertips. These sensors offer three-directional measurements using Hall effect sensing and embedded silicone. By controlling fingertip force based on information from the tactile sensors, the gripper achieves safe grasping. The gripper is evaluated to grasp daily life objects with different properties such as shapes, sizes, and levels of deformability. Evaluation results showcase the gripper's versatility, enabling it to securely grasp various objects, including fragile items. This outcome underscores the gripper's effectiveness, versatility, and safety in practical use.

Keywords: gripper design; open-source robotics; soft skin fingertip sensor; safe grasping.

I. Introduction

The gripper is a critical component of a robot, serving as the robot's hand for direct interactions with the outside world, such as touching, picking, grasping, analyzing, and manipulating objects [1][2]. In industrial settings, dealing with known and rigid objects makes grasping relatively straight forward, with less need for precise force control [3]. However, applying this in non-industrial environments can be challenging, as it may lead to mishandling and damage due to variations in object properties [4][5].

A proper design of the gripper significantly contributes to the success of the robot task. Generally, there are two types of gripper design based on the number of fingers: two-fingered hand, and multi-fingered hand [6][7]. Two-fingered hands are widely adopted due to their simplicity in control, cost-effectiveness, and high payload capacity. Companies like Schunk offer commercial grippers of this type. In contrast, multi-fingered hands aim to replicate the versatility and dexterity of human hands. This category includes a three-fingered hand (e.g., Barret Hand, Robotiq), a four-fingered hand (e.g., SMC, Festo), or an anthropomorphic hand (e.g., Shadow Dexterous Hand, Allegro Hand) [8][9]. In these gripper types, each phalanx possesses its actuator, enabling independent movement. As a result, these grippers can grasp and manipulate a

* Corresponding Author. Tel: +62-812-3328-0920
E-mail address: muha204@brin.go.id, muhtadin@ee.its.ac.id

doi: https://dx.doi.org/10.14203/j.mev.2023.v14.114-126

MEV is Scopus indexed Journal and accredited as Sinta 1 Journal (https://sinta.kemdikbud.go.id/journals/detail?id=814)
How to Cite: M. Arifin *et al.*, "An open-source parallel gripper with an embedded soft skin fingertip sensor," *Journal of Mechatronics, Electrical Power, and Vehicular Technology*, vol. 14, no. 2, pp. 114-126, Dec. 2023.

wide range of objects. To simplify control in the face of increasing complexity, underactuated mechanisms were introduced. These mechanisms allow grippers to adapt their grasp depending on the contact region. However, despite their capabilities, these commercially available grippers are often prohibitively expensive and only provide the hardware without integrated soft skin sensors for sensitive objects. This necessitates additional expenses and modifications. This issue can be a significant barrier, particularly for entry-level robotic researchers who face different conditions in their respective regions.

As an alternative, open-source designs offer an option to create inexpensive grippers for research and education [10]. Nurpeissova *et al.* used a mechanical linkage, a gear train, and an extension spring to create a multi-fingered hand. This gear-train transmission allows the control of all fingers with a single actuator [11]. Reference [12] developed the PG2 gripper with the ability to grasp, twist, and sense contact force with a series elastic actuator mechanism. Reference [13] presented an adaptive finger that is capable of enveloping or pinching grasp by using a Hart's linkage and a parallelogram linkage mechanism. Despite the fact that the designs were entirely open to everyone, they are prohibitively difficult to assemble since the gripper contains a lot of parts and a special element that needs to be taken into consideration, such as spring, tendon, gear, etc. Moreover, ensuring that these special elements have the correct parameters, like spring constant (K), as specified in the original design, can be complex. Mismatches in these parameters may lead to interference within the mechanism. Finding the precise parameters for these special elements can also be difficult in some regions. On the other hand, a two-fingered hand with a linear guide mechanism or parallel four-bar mechanism is known for its simple construction and cost-effectiveness when compared to other gripper designs [14][15][16]. However, to the best of the authors' knowledge, a complete compact design with a complete feature, open control software with built-electronics, and ready-to-use in grasping and manipulating applications, is not available. Some modifications are still required to reach the same quality research level as the other researchers who use commercial grippers and this task takes a long time to prepare. Furthermore, there is no guarantee of safety when using these open-source grippers, as most of them only provide mechanical designs without integrated safety features.

Recent advancements in gripper technology have garnered significant attention in the quest for safe and gentle interactions with various objects. One common approach to achieving this is to integrate cameras, force sensors, or tactile sensors into commercially available grippers, allowing them to perceive object properties during grasping and manipulation [17][18][19]. Some researchers presented vision-based control to localize and pick the object in a cluttered box using deep learning [20]. While these systems achieve a high success rate in picking, handling delicate objects remains a challenge. Soft robotic grippers have been developed to gently grasp objects with a simple open-loop control mechanism [21][22]. However, constructing such grippers can be complex and may require specific tools. Additionally, these grippers lack the capability to recognize and analyze objects during the grasping process as they lack feedback mechanisms. On the other hand, safe grasping is not only getting in contact with the object but also considering the object's properties to prevent slip and damage caused by over-force grasping.

Integrating tactile sensing as a sense of touch to gripper potentially improves object grasping. Tactile sensors provide valuable information about slip and object deformation based on contact forces [23]. Some studies have shown that shear forces in the x-axes and y-axes from tactile sensors play a significant role in detecting slips during grasping, while normal force in the z-axis helps assess object deformation [24]. The slip and object deformation states are classified using a machine learning algorithm. Each finger is equipped with uSkin, a distributed tactile sensor that offers 24 sensor points to collect the object's contact force [25]. Commercially available tactile sensors like Gelsight and Contactile are also available [26][27]. However, to ensure the gripper is affordable, accessible, and easy to build, employing a single-point 3-axis tactile sensor as a state control mechanism is sufficient for safe grasping.

This work presents a complete gripper design employing a parallel four-bar linkage mechanism, making it freely available and accessible for research and educational purposes. The design features minimal part numbers and utilizes a lot of off-the-shelf components and ease of construction, resulting in a low-cost platform that can be quickly assembled. To extend the gripper's ability, the fingertip part is also integrated with a soft skin tactile sensor. The tactile sensor provides three-directional in normal and shear forces data based on Hall effect sensing. This tactile sensor is used as the sense of touch of the gripper to control the grasping and to analyze the object based on contact force. This paper showcases the gripper's ability to safely handle unknown and delicate objects (Figure 1).

This study has the following contributions:

- A complete design with a very low-cost and straightforward mechanism makes it more accessible and rapidly prototyping for everyone
- Incorporating the tactile sensor into the proposed gripper in a single package design to enhance its capability for safe grasping and object analysis
- An algorithm that enables the gripper to safely grasp unknown and delicate objects

The rest of this paper is organized as follows. Section II discusses the proposed methods including the gripper design, soft skin sensor, and architecture and hardware system. Section III presents the experimental results and discussions. Finally, section IV draws conclusion and discusses future work.

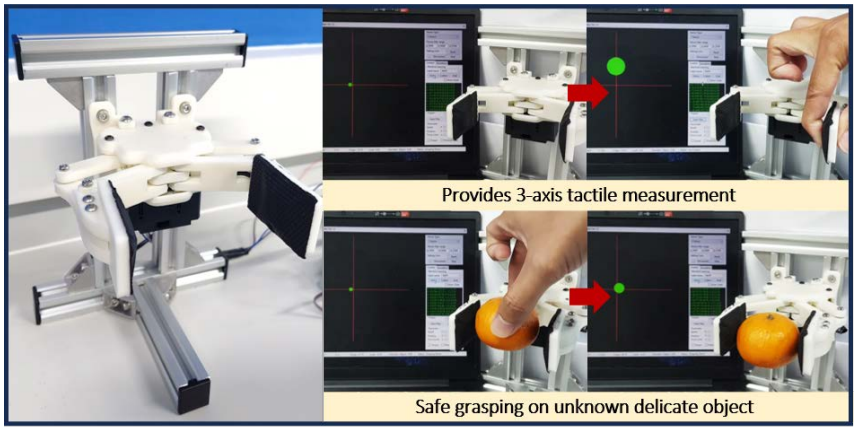

Figure 1. A compact gripper integrated with a 3-axis soft skin tactile sensor for safe grasping application and this gripper is affordable, accessible, and easy to build for research and educational purposes

II. Materials and Methods

A. Gripper design

The low cost and ease of fabrication are the main objectives to make grippers accessible for everyone. To fulfill this requirement, a two-finger based on parallelogram linkage is chosen for the driven mechanism of the gripper. The parallelogram linkage is the simplest mechanism that keeps the finger's orientation with a minimum link. The parallelogram linkage works based on Grashof's rule, which exploits a four-bar in the form of quadrilateral linkage as seen in Figure 2. Depending on how the four bars are configured, there are various cases of motion produced to the output link. To establish the parallelogram linkage, the four-bar must fulfill this requirement as equation (1).

$$s + l = p + q \tag{1}$$

where s, l, p, and q is the input link, coupler link, output link, and frame link, respectively. Four revolute pairs connect these members, forming a closed-loop kinematic chain with a single degree of freedom. Designing the four-bar linkage in this manner allows for the creation of a parallel gripper. Each finger employs the parallelogram linkage with distinct input motions. To achieve synchronized parallel movement of the two fingers, it is essential to ensure that the two input motions are coordinated.

There was a method to synchronize the two fingers based on rack and pinion [28]. This approach involved the use of a lead screw to drive the rack and pinion with a single actuator. However, in line with our goal of creating a simplified gripper with fewer components, we opted for a straightforward gear train transmission system. This gear train comprises two spur gears with identical teeth sizes: a driver gear and a driven gear. This driver gear is fixed to the actuator and transmits the motion and force to the driven gear in opposite directions. As a result, connecting the driver gear to the input joint of the left finger and the driven gear to the right finger ensures that both fingers move in parallel. Furthermore, this mechanism also allows the two fingers to be actuated by a single actuator, lowering the cost and control complexity. Figure 3 depicts the gear train system including the parallelogram linkage. The proposed gripper is assembled with one parallelogram linkage for each finger, both driven by a single actuator. The gripper possesses 1 degree of freedom (DoF), which can be fully controlled to open and close with parallel movements.

The kinematic analysis of the gripper is shown in Figure 4. Table 1 provides an overview of the D– H parameters for the finger. Here, l_i represents the length of linkage i, with i taking values of 1, 2, and 3. The parameter d_i indicates the distance between connected joints from X_{i-1} to X_i, along the Z_i axis. Additionally, α_i denotes the coupler angle from Z_{i-1} to Z_i, in the forward direction of the X_{i-1} axis (representing the torsion angle of linkage i). Lastly, θ_i denotes the joint angle from X_{i-1} to X_i, in the forward direction of the Z_i axis (indicating the rotation angle between linkage $i-1$ and linkage i).

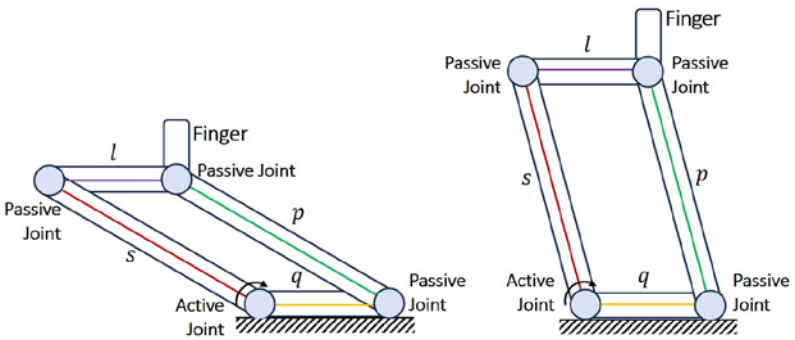

Figure 2. A Mechanism of the four-bar linkages, the finger's orientation remains constant in any position

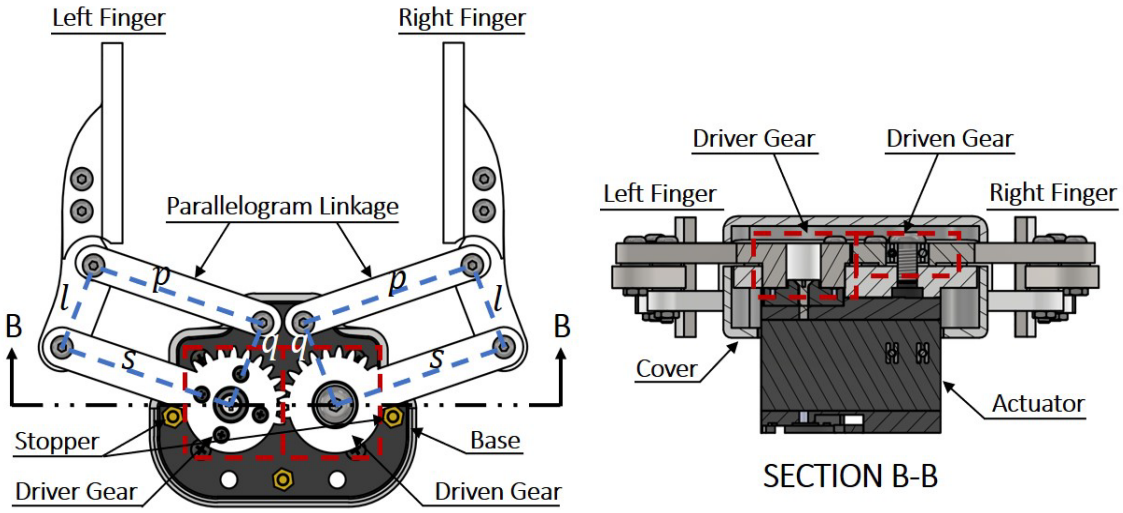

(a) (b)

Figure 3. Gear train (red dotted line) and parallelogram linkage (blue dotted line) of the proposed gripper: (a) Top-view without top cover; (b) Half-section view of the internal mechanism

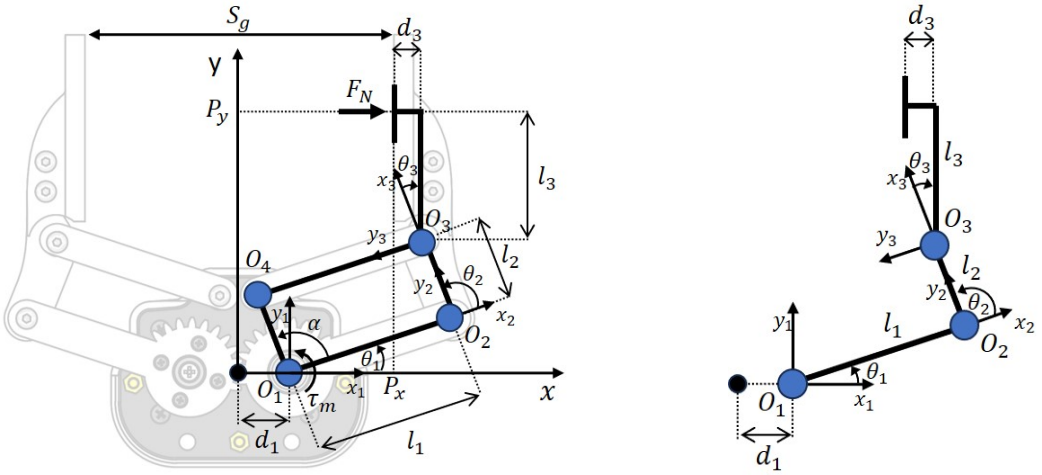

(a) (b)

Figure 4. Kinematics model: (a) Gripper system; (b) Simplified system

The expression for the homogeneous transformation matrix between two connecting rods adjacent to each other is given by equation (2).

$$ {}^{i-1}_{i}T = \begin{bmatrix} \cos\theta_i & -\sin\theta_i \cos\alpha_i & \sin\theta_i \sin\alpha_i & L_i \cos\theta_i \\ \sin\theta_i & \cos\theta_i \cos\alpha_i & -\cos\theta_i \sin\alpha_i & L_i \sin\theta_i \\ 0 & \sin\alpha_i & \cos\alpha_i & d_i \\ 0 & 0 & 0 & 1 \end{bmatrix} \quad (2) $$

where ${}^{i-1}_{i}T$ is the transformation matrix between linkage $i-1$ and linkage i.

Hence, the coordinates position of the gripper in the fundamental coordinate system can be represented as equation (3).

$$ \begin{bmatrix} P_x \\ P_y \\ P_z \\ 1 \end{bmatrix} = \begin{bmatrix} l_1 c_1 + l_2 c_{12} + l_3 c_{123} + d_1 - d_3 \\ l_1 s_1 + l_2 s_{12} + l_3 s_{123} \\ 0 \\ 1 \end{bmatrix} \quad (3) $$

where P_x, P_y, P_z, l_1, l_2, l_3, d_1, and d_3 are finger position in cartesian x-coordinates, finger position in cartesian y-coordinates, finger position in cartesian z-coordinates, the distance link 1 between O_1 and O_2, the distance link 2 between O_2 and O_3, the distance link 3 between O_3 and the finger, the offset length of link 1, and the offset length of link 3, respectively. Here, s_{ijk} and c_{ijk} represent the $\sin(\theta_i + \theta_j + \theta_k)$ and $\cos(\theta_i + \theta_j + \theta_k)$, respectively.

Table 1.
D-H parameters of the proposed finger

Link	$\boldsymbol{\theta_i}$	$\boldsymbol{\alpha_i}$	$\boldsymbol{L_i}$	$\boldsymbol{d_i}$
1	θ_1	0	L_1	d_1
2	θ_2	0	L_2	0
3	θ_3	0	L_3	d_3

The gripper's motion is separated into two stages: grabbing and releasing. The limit of the motion gripper depends on the kinematic parameter in equation (3). The stroke length can be derived from the finger position on the x-axis. Since the parallel gripper keeps the finger's orientation, the relationship between θ_1, θ_2, and θ_3 are expressed as equation (4).

$$\theta_1 + \theta_2 + \theta_3 = 90° \tag{4}$$

The θ_1 is the active joint driven by the actuator while the θ_3 is mechanically fixed at 21.8°. Hence, the θ_2 can be rearranged as equation (5).

$$\theta_2 = 111.81° - \theta_1 \tag{5}$$

By substituting (5) into (3), the stroke length can be derived as equation (6).

$$S_g = (l_1 c_1 - 0.37 l_2 + d_1 - d_3) * 2 \tag{6}$$

where S_g is the stroke length of the gripper.

When the gripper makes contact with the object, it Sresults in the generation of interacting forces and torques between the finger and the object. The key condition for achieving stable grasping is that the net force acting on the object is equal to 0 [29]. As per equation (3), we convert it into matrix form:

$$\begin{bmatrix}\delta P_x \\ \delta P_y\end{bmatrix} = \begin{bmatrix}\frac{\partial P_x}{\partial \theta_1} & \frac{\partial P_x}{\partial \theta_2} & \frac{\partial P_x}{\partial \theta_3} \\ \frac{\partial P_y}{\partial \theta_1} & \frac{\partial P_y}{\partial \theta_2} & \frac{\partial P_y}{\partial \theta_3}\end{bmatrix}\begin{bmatrix}\delta\theta_1 \\ \delta\theta_2 \\ \delta\theta_3\end{bmatrix} = \boldsymbol{J}\begin{bmatrix}\delta\theta_1 \\ \delta\theta_2 \\ \delta\theta_3\end{bmatrix} \tag{7}$$

$$J = \begin{bmatrix}-l_1 s_1 - l_2 s_{12} - l_3 s_{123} & -l_2 s_{12} - l_3 s_{123} & -l_3 s_{123} \\ l_1 c_1 + l_2 c_{12} + l_3 c_{123} & l_2 c_{12} + l_3 c_{123} & l_3 c_{123}\end{bmatrix} \tag{8}$$

where J represents the velocity Jacobian matrix of the proposed gripper. The determination of the Jacobian matrix J is guided by equation (3) and equation (7). Simplifying equation (7) yields

$$\dot{X} = J(q)\dot{q} \tag{9}$$

where $q = [\theta_1, \theta_2, \theta_3]$, and $\dot{X} = [\dot{P}_x, \dot{P}_y]$.

Throughout the gripper's grasping process, there is no displacement of the force acting on the object. Adhering to the principle of virtual work [30], the equilibrium equation is articulated as:

$$\tau = J^T F \tag{10}$$

where τ and F signify joint torque and the contact force between the linkage and the object.

The dynamic model establishes a connection between the input actuation torque and the resulting motion of the gripper, playing a crucial role in the systematic design and control of the gripper. The Lagrangian for this proposed gripper is expressed as equation (11):

$$\mathcal{L} = \mathcal{T} + \mathcal{U} \tag{11}$$

where $\mathcal{L}$, $\mathcal{T}$, and $\mathcal{U}$ represent Lagrangian function, total kinetic energy and total potential energy, respectively. The kinetic energy is derived as equation (12) and equation (13):

$$\mathcal{T} = \frac{1}{2}\dot{q}^T M(q)\dot{q} \tag{12}$$

$$M(q) = \left[\sum_{i=1}^{3}\{m_i J_v^i(q)^T J_v^i(q) + J_w^i(q)^T R_i(q) I_i R_i(q)^T J_w^i(q)\}\right] \tag{13}$$

In this context, $M(q)$, m_i, R_i and I_i denote the generalized inertia matrix, the mass of link i, rotation matrix and inertia matrix of link i, respectively. The linear and angular velocity Jacobians of link i, denoted as $J_v^i(q)$ and $J_w^i(q)$, can be expressed as equation (14).

$$J_v^i = [J_{v1}^i \dots J_{vi}^i 0 \dots 0],\ J_w^i = [J_{w1}^i \dots J_{wi}^i 0 \dots 0] \tag{14}$$

where $J_{vj}^i = z_j\, x\, (p_{li} - p_j)$, $J_{wj}^i = z_j$, and z_j represents a unit vector along the direction of joint j, employed for calculating the linear, and angular velocity Jacobians of link i, respectively. The linear and angular velocity Jacobians of the proposed gripper are expressed as equation (15) and equation (16).

$$J_v = \begin{bmatrix}-(l_1 s_1 + l_2 s_{12}) & -l_2 s_{12} & 0 \\ l_1 c_1 + l_2 c_{12} & l_2 c_{12} & 0 \\ 0 & 0 & 0\end{bmatrix}\begin{bmatrix}\dot{\theta}_1 \\ \dot{\theta}_2 \\ \dot{\theta}_3\end{bmatrix} \tag{15}$$

$$J_w = \begin{bmatrix}0 & 0 & 0 \\ 0 & 0 & 0 \\ 1 & 1 & 1\end{bmatrix}\begin{bmatrix}\dot{\theta}_1 \\ \dot{\theta}_2 \\ \dot{\theta}_3\end{bmatrix} \tag{16}$$

The potential energy can be formulated as equation (17).

$$\mathcal{U} = \sum_{i=1}^{3} m_i g^T p_{li} \tag{17}$$

with g and p_{li} representing the gravitational vector and the position vector of the mass center of link i, respectively. The equations of motion for this finger's gripper are then determined as equation (18).

$$\frac{d}{dt}\left(\frac{\partial \mathcal{L}}{\partial \dot{q}_i}\right) - \left(\frac{\partial \mathcal{L}}{\partial q_i}\right) = \tau_i \tag{18}$$

Overall, the presented gripper is comprised of a single actuator, 42 commercial off-the-shelf (COTS) components (including bolts, nuts, bearings, etc.), one sensor, and 11 printed parts. These printed parts include four components for each finger, incorporating the spur gears, one base part, and two cover parts. The CAD 3D model of the proposed gripper is created using Autodesk Inventor. All printed parts including spur gears are created through 3D printing with acrylonitrile butadiene styrene (ABS) filament using the Prusa i3 MK3S+, a commercial 3D printer. The majority of parts are designed to have flat surfaces for ease of printing without needing a lot of support and effort. The printed part and the assembly model of the gripper are presented in Figure 5. The active rotational joint is connected directly to the actuator while the other passive rotational joints are linked through pivots with sleeve bearings. Both fingers are actuated by a single actuator using the gear train transmission, resulting in parallel motion with synchronized movement for both fingers. Even though this gear train transmission produces more backlash, this gripper has the fewest parts and does not have any special elements such as spring or tendon, so assembling this gripper is straightforward and does not require a skilled mechanical engineer. Most importantly, this gripper can be rapidly constructed

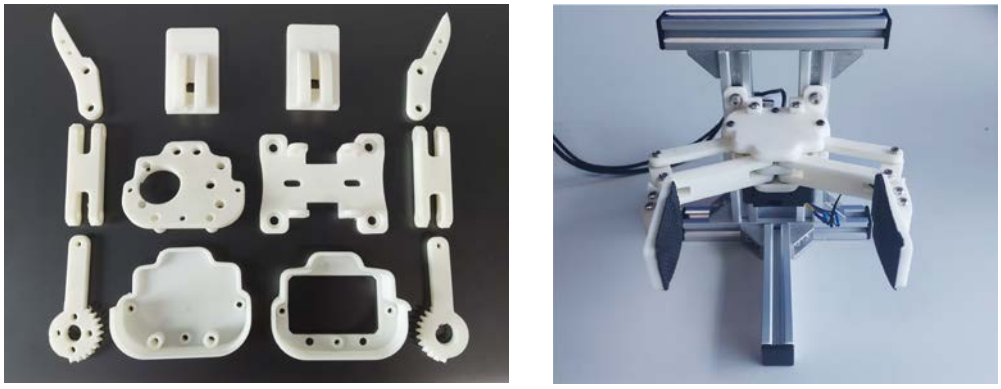

(a) (b)

Figure 5. The two-fingered gripper assembly model: (a) Printed parts; (b) 3D-printed prototype

and is ready for use in a wide range of robotic applications.

B. Soft skin fingertip design

The tactile sensor is based on uSkin technology which was published in [25]. The sensor provides normal and shear forces based on the hall effect with the soft skin. This sensor consists of a soft elastomer, a permanent magnet, and a magnetic field sensing element. The small permanent magnet is centrally positioned above the magnetic field sensing element, with both parts embedded within the soft material, as shown in Figure 6. Under normal circumstances, the Hall effect detects the magnetic field emitted by the permanent magnet. When the soft material is deformed due to the external force from the outside, the displacement of the permanent magnet changes and the Hall effect sensor captures magnetic field variations. These changes in magnetic fields are then translated into x-axis, y-axis, and z-axis forces. Calibration is essential to convert the magnetic field alterations into force measurements.

The soft fingertip sensor has three layers in total. The bottom layer is the PCB for the magnetic field sensing element. A tri-axis magnetometer from Melexis, MLX90393, is used as the magnetic field sensing element. The middle layer is made of silicone and serves as the container for the embedded permanent magnets, PCB, and chip. Liquid silicone rubber, specifically Ecoflex Supersoft from Smooth-On with a shore hardness of 00-30, is used for this purpose. The silicone is poured in the form of a cube trapezoidal using a molding cast, as shown in Figure 7. This molding cast is manufactured by using the 3D printer with the hole marker for an air gap and the permanent magnet.

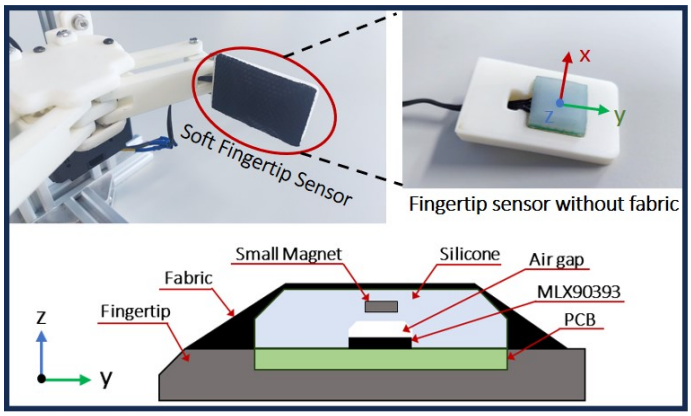

Figure 6. Soft skin tactile sensor based on Hall-effect sensing attached to the fingertip gripper

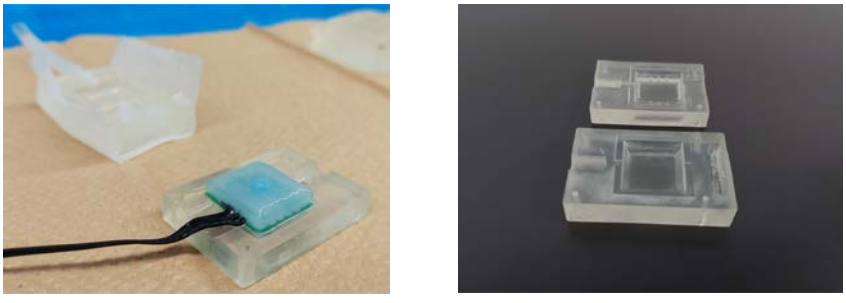

(a) (b)

Figure 7. (a) The liquid silicone rubber was poured and cured; (b) Printed molding cast

The layer incorporates an air gap structure between the Hall-effect sensor and the silicone to enhance sensitivity for small forces. The silicone layer is wider than the chip to cover the area detection of the fingertip. The top layer is a grip tape. The grip tape has a gecko-like structure to increase the friction for better grip, especially for slippery objects. This grip tape is glued on the top of the silicone and the fingertip. Overall, the sensor has a size of 18x18x6 mm. A single 3-axis tactile measurement for the proposed gripper is sufficient because the gripper's objectives are to produce a low-cost, straightforward design with excellent performance for grasping and analyzing the object.

C. Architecture and control system

The architecture system of the proposed gripper is depicted in Figure 8. A dynamixel with a series of XL430-W250 is utilized for the actuator of this gripper. This actuator streamlines the system by incorporating a comprehensive package consisting of the motor, reduction, encoder, sensor, and controller. The XL430-W250 boasts a stall torque of 1.5 Nm at 12 V and operates at a speed of 61 rpm under no-load conditions. Its compact dimensions make it an ideal choice for the proposed gripper. If necessary, it can be easily replaced with a higher-power alternative, such as the XM or XH series. The actuator is securely mounted on the base and directly drives the driver gear to operate both fingers. Furthermore, an OpenRB-150, a controller board from Robotis is utilized for the control electronic system of the gripper. This board is mainly designed to control the dynamixel with high power. The microcontroller is powered by a SAMD21 Cortex-M0+ 32-bit processor with a 48 MHz clock frequency. The board offers compatibility with various peripherals such as SPI, I2C, and UART, facilitating seamless integration with other sensors and actuators. The actuator is connected via TTL to this board. Notably, the actuator is configured with default settings (57600 bps, ID 0), obviating the need for any adjustments within the Dynamixel. Furthermore, the Dynamixel provides control commands to access the data and modify data as well to control the actuator, i.e., velocity control, position control, present position, present load, PID gain setting, etc. The present position is transformed to the present stroke by Equation (6).

The magnetic field data from the fingertip sensor is acquired through the I2C protocol and interfaced with this board. The sensor is set to the burst mode, which provides a 3-axis magnetic field measurement with a sampling rate of up to 500 Hz. To minimize the noise, a built-in digital filter from the sensor is also configured. The collected data is sent to the PC via UART. This data is useful to decide the control system of the gripper or to collect the data for object analysis using machine learning, for example. A graphical user interface (GUI) is provided to visualize the sensor and control the motion of the gripper. The user has access to move the finger to the specific stroke, monitor the actuator data, and the 3-axis soft fingertip sensor. Presently, this GUI is compatible with Windows, but there are plans to provide control access through the robot operating system (ROS) in the future.

The control system of the proposed gripper is designed with sophistication, incorporating PID controller for position control mode, as shown in Figure 9. The control system is based on the Dynamixel control table system. These advancements play a crucial role in governing the gripper's actions, ensuring precise and accurate control. The DYNAMIXEL bus receives user commands to initiate the procedure. These commands are meticulously recorded as the goal position, serving as the initial input for the gripper's movement. Subsequent phases in the control process involve converting the goal position into a desired position and velocity trajectory using the profile velocity and profile acceleration parameters.

The resulting trajectories are stored in designated memory locations: position trajectory and velocity trajectory. These stored values act as reference points for the gripper's subsequent motion, providing a foundation for comparison and adjustment throughout the control process. The system utilizes PID controllers to achieve accurate and responsive movements. These controllers

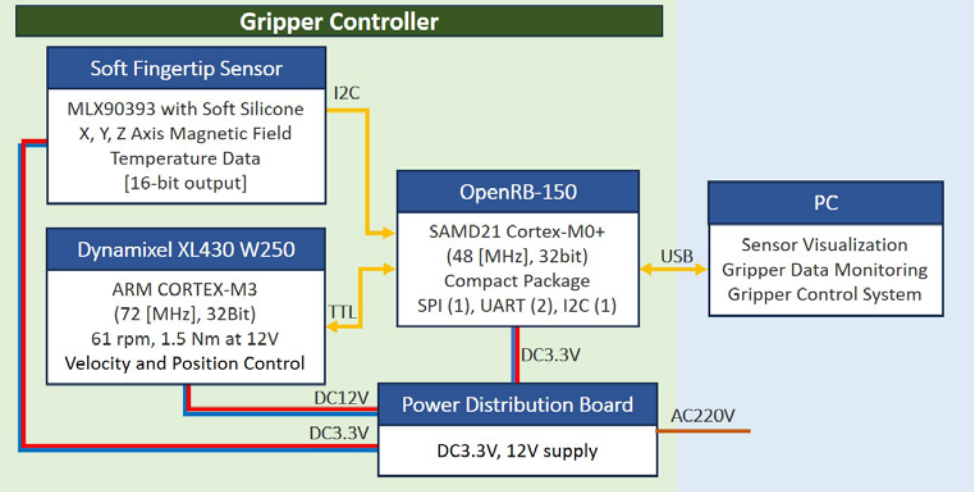

Figure 8. Architecture and hardware system

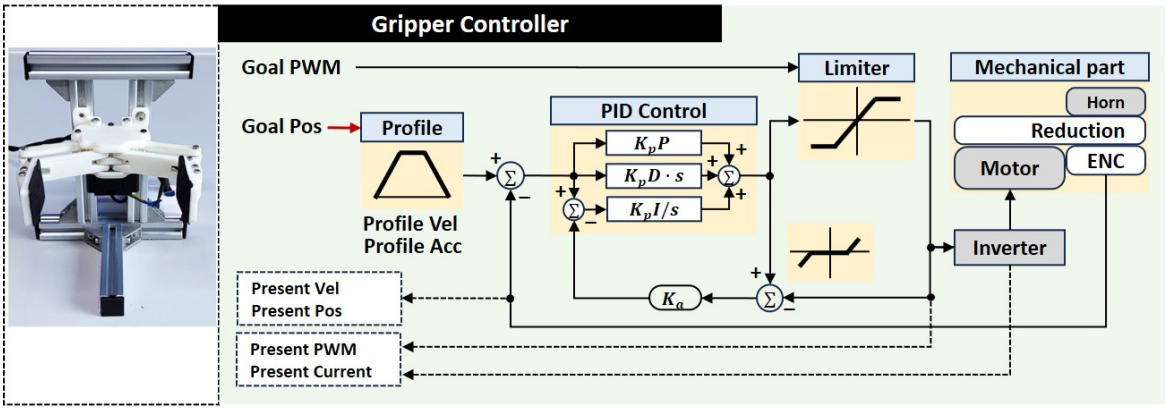

Figure 9. Architecture control system

collaborate to calculate the motor's pulse width modulation (PWM) output based on the required trajectories. The PWM output is further refined by applying the constraints of the Goal PWM, ultimately determining the final PWM value. This value is then transmitted to the motor through an inverter, driving the gripper's finger.

The outcomes of this intricate control process, including present position, present velocity, present PWM, and present load, are stored for subsequent analysis and feedback. This comprehensive feedback loop ensures that the gripper's motion is not only controlled in real-time but also adaptable to changes in the environment or task requirements. The system's flexibility extends to PWM Control Mode, where both PID controllers are disengaged. Instead, the motor is directly influenced by the Goal PWM value through an inverter. This mode provides users with direct control over the motor's supply voltage, offering a more flexible approach to gripper operation.

K_p, K_i, and K_d serve as the gains utilized in the PID controller of the proposed system. Achieving precise and responsive control necessitates the fine-tuning of these PID gains. K_p (proportional gain) influences the system's response, with a small value potentially leading to a slow response time, while an excessively large value may induce instability, such as oscillation. K_d (derivative gain) contributes to improving settling time and stability by dampening overshoot. K_i (integral gain) aids in reducing steady-state error, the residual discrepancy between the goal and present positions. Fine-tuning PID settings enhances the accuracy and responsiveness of actuator control, addressing position errors as well. In this study, the K_p, K_i, and K_d gains are configured as 800, 0, and 0, respectively. Notably, since the Dynamixel actuator incorporates a velocity controller with proper PI gain (K_p = 100, K_i = 1920, K_d = 0), determining suitable PID gains for the position mode proves to be a straightforward process and setting the proportional gain (K_p) for the position control of the gripper is sufficient.

The inclusion of the anti-windup gain (K_a) is another critical component. While not user-modifiable, this parameter plays a crucial role in enhancing stability and preventing issues related to windup. The anti-windup gain contributes to the overall robustness of the gripper's control system, ensuring a smooth and steady control operation.

III. Results and Discussions

In this section, the gripper's performance including the soft skin sensor and the safe grasping on unknown and delicate objects are evaluated.

A. Gripper performance

We assess the performance of the proposed gripper's ability to grasp objects of varying shapes and sizes. The experiments encompassed objects of diverse shapes and sizes to assess the gripper's versatility in handling different geometries. Notably, for this evaluation, we excluded the use of the tactile sensor to concentrate solely on the gripper's performance in reliably grasping objects. We selected a range of objects, including small items such as pens and bottle caps, medium-sized objects like a cutter and tape, and irregularly shaped objects resembling household items and tools. These objects were chosen to challenge the gripper's adaptability to different shapes and sizes commonly encountered in everyday scenarios. Stability during grasping was also evaluated based on the absence of slipping or dropping of objects. We conducted 5 trials for each object to ensure the reliability of the results. The experiments were carried out under controlled conditions to isolate the gripper's performance without considering external factors such as environmental disturbances or object deformations.

Figure 10 shows that the gripper demonstrated remarkable performance across all tested objects, indicating the gripper's reliability in handling different shapes and sizes. Minimal instances of slipping or dropping objects were observed, demonstrating the gripper's stability during grasping. The addition of grip tape to the gripper's fingertip sensor increased friction, resulting in fewer instances of slipping or dropping objects while grasping. The gripper's ability to handle a wide range of geometries with such consistency opens up possibilities for its application in tasks requiring intricate object manipulation. Furthermore, the proposed gripper is compared to existing gripper models in terms of key performance parameters such as mass, stroke length, and cost. This comparison is shown in Table 2.

Figure 10. Grasping of objects with different shapes and sizes using the proposed gripper

The proposed gripper has a significantly lower mass, a competitive stroke length, a substantial gripping force, and a reasonable price of $98, making it a feasible choice for research and educational applications. Existing grippers have varying specifications to meet the needs of the robotics community. A detailed breakdown of component costs is shown in Table 3. This figure encompasses essential components such as the Actuator Dynamixel XL430-W250, Controller Board OpenRB-150, and various 3D-printed parts. This brief comparison highlights the proposed gripper's advantages in terms of compactness, affordability, and performance, establishing it as a valuable addition to the field.

B. Soft skin fingertip sensor performance

The soft skin sensor performance is evaluated in this section. The experiment is conducted on the repeatability and sensor response in a real scenario when the gripper grasps the object. In this experiment, the gripper is configured to apply force with pushing movement to a cylindrical 3D print attached to a reference sensor. To validate the response of the soft skin sensor, a calibrated strain gauge sensor is employed as the reference. This reference sensor measures the normal force, so this section specifically assesses the z-axis of the soft skin sensor, while the x-axis and y-axis data are retained. In certain applications, knowing the direction of applied shear forces (x-axis and y-axis) is sufficient for slip analysis and safe manipulation using machine learning, for example. The data from the reference sensor is recorded with an Arduino Uno and synchronized for sensor analysis. To prepare the sensor for measurement, it is necessary to offset the readout data by subtracting it from the baseline.

Figure 11 displays the response of the soft skin sensor alongside its reference sensor when subjected to a constant force. The soft skin sensor measured the same trend force as the reference sensor. The repeatability test was also conducted with 4 cycles by releasing and pushing the cylindrical part with the same force, and the soft skin sensor consistently yielded results across these cycles. The output was also returned to zero when the gripper released the pushing force. During the normal force test, some

Table 2.
Gripper comparison

Gripper	Mass (g)	Stroke (mm)	Cost ($)	Mechanism
Sake EZ gripper	365	145	2,500	Tendon underactuated
Robotis RH-P12-RN	500	106	3,186	Mechanically underactuated
DH robotics AG-95	1,000	95	3,900	Mechanically underactuated
Robotiq 2-finger 85	890	85	4,800	Mechanically underactuated
Blue gripper	660	126	328	Parallel linkage
Baxter easyhand	NM	80	150 + NM*	Tendon & parallel
InstaGrasp	660	126	108**	Tendon underactuated
Proposed gripper	154	120	98	Parallel linkage

Table 3.
Final cost of the proposed gripper

Component	Quantity	Total Cost ($)
Actuator dynamixel XL430-W250	1	49.90
Controller board openRB-150	1	24.90
Base part 3D-printed	1	0.60
Cover part 3D-printed	2	1.10
Finger part 3D-printed	8	2.00
Bolts, nuts, bearing, etc.	1	9.50
Sensor (permanent magnet, chip, component)	1	5.00
Liquid silicone rubber	1	5.00
Total		98.00

displacement occurred in the x-axis and y-axis. This displacement can be attributed to the arc trajectory motion of the parallel gripper resulting from the parallel linkage mechanism. This motion occasionally leads to a sideway push effect on the sensor, even though the gripper's primary motion is parallel. It is shown that the x-axis and y-axis also contribute to the proposed parallel gripper. This behavior possibility happens when using another commercial parallel gripper, such as robotiq. Additionally, the placement of the magnet may be a contributing factor, as it is manually positioned and may not always be perfectly centered.

For calibration, the soft skin sensor was subjected to stepwise increasing forces in a six-step process, with each step maintained for six seconds at a constant force. Figure 12 displays the responses of both the soft skin sensor and the reference sensor. The soft skin sensor closely mirrored the trendline observed in the reference sensor, effectively tracking the changes in force. The displacement of the x-axis sensor happens due to the arc trajectory motion of the parallel gripper as well. This leads to a sideway push effect on the sensor. In Figure 13, the calibrated response of the soft skin sensor is presented. In this experiment, the same stepwise forces were applied, but the gripper was released for 6 seconds before moving on to the next force level. The results indicate that the sensor's output closely corresponds to that of the reference sensor and returns to zero during the release movement.

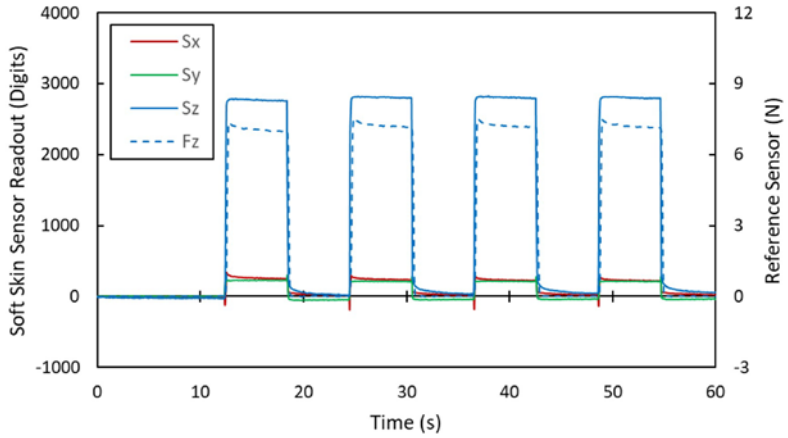

Figure 11. Soft skin sensor's readout and the corresponding force from reference sensor with repetitive test (S = sensor, F = reference sensor)

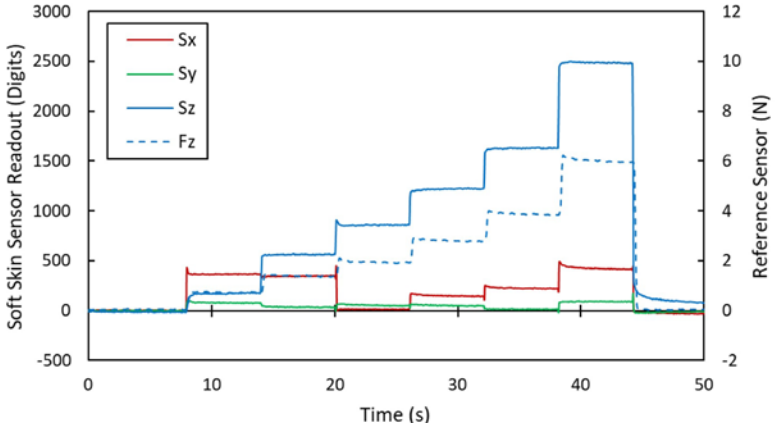

Figure 12. Sensor response on stepwise z-axis force

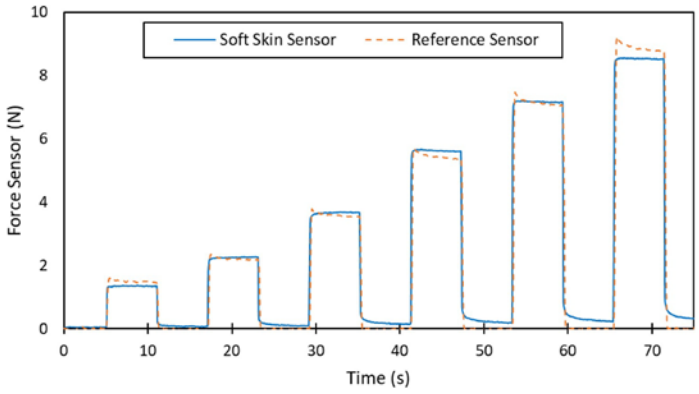

Figure 13. Calibrated sensor and the corresponding force from reference sensor on stepwise force

C. Safe grasping of unknown and delicate objects

This section demonstrates the safe grasping of unknown and delicate objects using the soft skin sensor. In our previous experiment, we showcased the limitations of conventional grasping when dealing with fragile items. Specifically, we used a plastic cup as a representative object, and the object was noticeably damaged during the grasping process, as shown in Figure 14(a). By utilizing the soft skin sensor attached to the gripper's finger as a feedback mechanism, we significantly improved the safety and efficacy of object grasping and handling. The sensor's sensitivity in measuring forces along the 3-axis directions allowed the gripper to securely grasp the object, preserving its shape and preventing slippage as showcased in Figure 14(b).

The gripper's finger is controlled according to the feedback from the soft skin sensor. The sequence of movements executed by the gripper is displayed in Figure 15. The graph shows the 3-axis measurement from the soft skin sensor and the current stroke length of the gripper during grasping. The y-axis on the left corresponds to the soft skin sensor's readings (red line, green line, and blue line), while the y-axis on the right is dedicated to the gripper's stroke length (orange line). Furthermore, the x-axis shows the sequential time frames, providing a coherent chronology of the grasping process. Initially, there was no response from the sensor since the gripper was on standby and did not move. Subsequently, as the gripper initiated finger closure and made contact with the object, the 3-axis measurements from the soft skin sensor changed significantly as shown in the plot. During grasping, the soft skin sensor measures a stable response, signifying that the object remained securely in place and did not drop. Once the object was released, another contact change was observed and the soft skin sensor readings returned to baseline.

According to the graph, the y-axis consistently demonstrated higher values than the other axes, indicating the potential for object slippage. It's important to note that applying excessive gripper force can achieve stable grasping and minimize object slippage, but it can crush the object. Therefore, controlling the gripper considering the risk of slippage from the y-axis and the grasping force from the z-axis is important. By leveraging the information provided by the soft skin sensor, the gripper can make a decision to control the finger for safe grasping. In addition, the x-axis data from the soft skin sensor is valuable for considerations related to the object's center of mass, enhancing grasp stabilization and object manipulation.

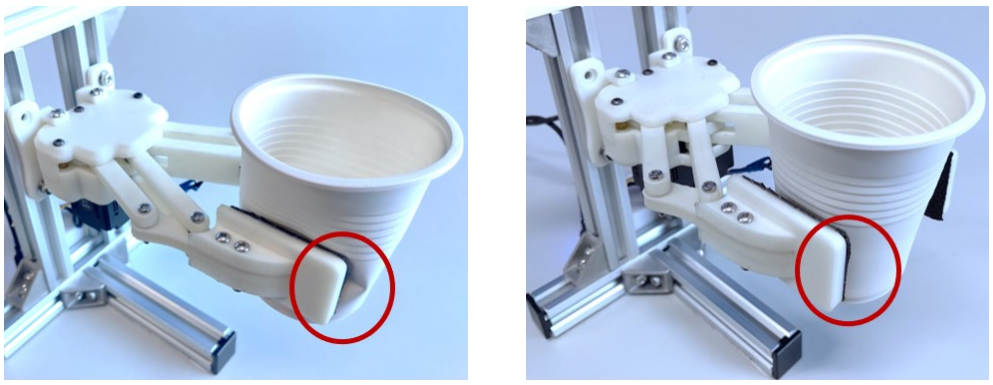

(a) (b)

Figure 14. (a) Conventional grasping with the fixed torque; (b) Safe grasping with the controlled finger based on a soft skin sensor

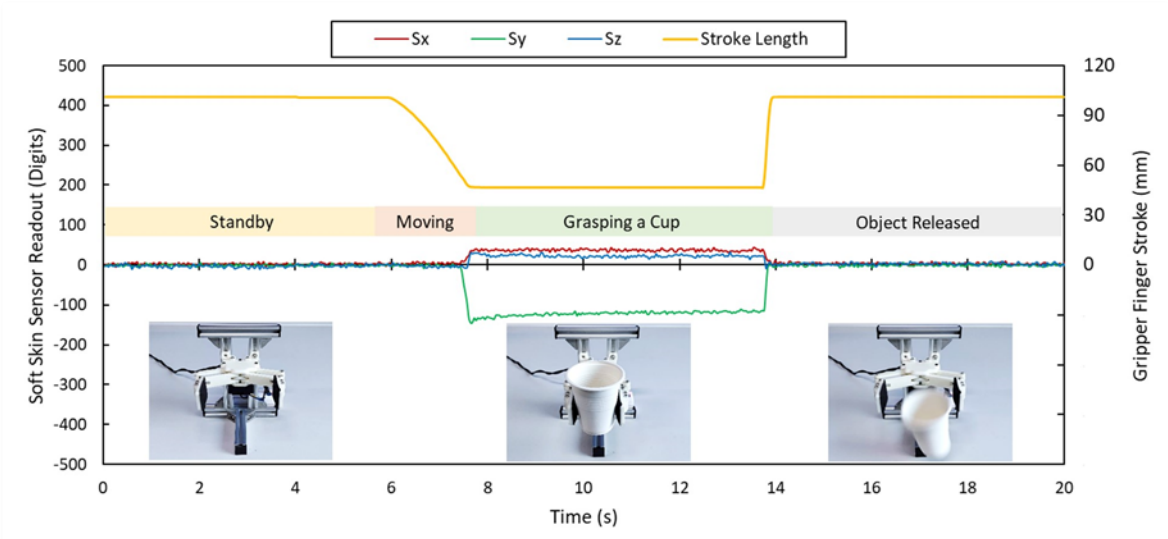

Figure 15. Sequential response of safe grasping

IV. Conclusion

This paper introduced a cost-effective and versatile gripper with an integrated soft skin sensor. The gripper demonstrated exceptional performance in grasping various objects, showcasing its stability and adaptability. Furthermore, the soft skin sensor exhibited reliability in measuring normal and shear forces. Its integration enhanced a layer of intelligence, enabling a safe grasping of unknown and delicate items, preserving their integrity and minimizing slippage or dropping. The 3-axis measurements from the soft skin sensor provided sensitivity and real-time information on the grasping process, allowing for precise control of the gripper's finger movements. This development addresses a significant challenge in robotics. The CAD model of the proposed gripper is available and accessible at https://github.com/muhaarifin/bripper_resources-.git. The straightforward assembly process and high-quality standard gripper address a critical barrier for entry-level researchers and educators, making it an attractive choice for those entering the field of robotics. As robotics technology continues to expand into our daily lives, the availability of accessible and capable grippers like the one presented here will play a vital role in advancing the field and fostering innovation.

Acknowledgements

We want to thank Tito Pradhono Tomo who explained the concept of making uSkin sensor and Tommy Pratama who helped analyze the gripper's model. We also want to thank Leonardo Fajar Mardika, Asany Herdiana, and Arya Bima Prastowo who helped prepare the experimental setup.

Declarations

Author contribution

M. Arifin: Writing - Original Draft, Writing - Review & Editing, Conceptualization, Formal analysis, Investigation, Visualization, Supervision. R.P. Pratama: Conceptualization, Software, Data Curation, Investigation. O. Mahendra: Conceptualization, Electronics, Validation. A. Munandar: Conceptualization, Software, Visualization. C.H.A.H.B. Baskoro: Writing - Review & Editing, Formal analysis. M. Muhtadin: Conceptualization, Supervision. A. Iskandar: Supervision.

Funding statement

This research was partially supported by the Home Program of Artificial Intelligence, Big Data, and Computing Technology for Biodiversity and Satellite Imagery 2023 No. 123, The Research Organization for Electronics and Informatics, National Research and Innovation Agency (BRIN).

Competing interest

The authors declare that they have no known competing financial interests or personal relationships that could have appeared to influence the work reported in this paper.

Additional information

References

[1] L. D. Evjemo, T. Gjerstad, E. I. Grøtli, and G. Sziebig, "Trends in Smart Manufacturing: Role of Humans and Industrial Robots in Smart Factories," *Current Robotics Reports*, vol. 1, no. 2, pp. 35– 41, Jun. 2020.

[2] G. Haidegger and I. Paniti, "Episodes of Robotics and Manufacturing Automation Achievements from the Past Decades and Vision for the Next Decade." Acta Polytechnica Hungaria: Journal of Applied Sciences, vol. 16, no. 10, pp. 119– 136, 2019.

[3] J. Arents and M. Greitans, "Smart Industrial Robot Control Trends, Challenges and Opportunities Within Manufacturing," *Applied Sciences (Switzerland)*, vol. 12, no. 2. MDPI, Jan. 01, 2022.

[4] T. Haidegger, P. Galambos, and I. J. Rudas, "Robotics 4.0 – Are we there yet?," in *2019 IEEE 23rd International Conference on Intelligent Engineering Systems (INES)*, IEEE, Apr. 2019, pp. 000117– 000124.

[5] B. Zhang, Y. Xie, J. Zhou, K. Wang, and Z. Zhang, "State-of-the-art robotic grippers, grasping and control strategies, as well as their applications in agricultural robots: A review," *Computers and Electronics in Agriculture*, vol. 177. Elsevier B.V., Oct. 01, 2020.

[6] Z. Samadikhoshkho, K. Zareinia, and F. Janabi-Sharifi, "A Brief Review on Robotic Grippers Classifications." in *IEEE Canadian Conference of Electrical and Computer Engineering (CCECE)*, pp. 1– 4, 2019.

[7] Z. Long, Q. Jiang, T. Shuai, F. Wen, and C. Liang, "A Systematic Review and Meta-analysis of Robotic Gripper," in *IOP Conference Series: Materials Science and Engineering*, Institute of Physics Publishing, Apr. 2020.

[8] Y. Li, P. Wang, R. Li, M. Tao, Z. Liu, and H. Qiao, "A Survey of Multifingered Robotic Manipulation: Biological Results, Structural Evolvements, and Learning Methods," *Frontiers in Neurorobotics*, vol. 16. Frontiers Media S.A., Apr. 27, 2022.

[9] S. Li *et al.*, "Vision-based Teleoperation of Shadow Dexterous Hand using End-to-End Deep Neural Network," in *2019 International Conference on Robotics and Automation (ICRA), IEEE*, May, pp. 416– 422, 2019.

[10] J. Hernandez *et al.*, "Current Designs of Robotic Arm Grippers: A Comprehensive Systematic Review," *Robotics*, vol. 12, no. 1. MDPI, Feb. 01, 2023.

[11] A. Nurpeissova, T. Tursynbekov, and A. Shintemirov, "An Open-Source Mechanical Design of ALARIS Hand: A 6-DOF Anthropomorphic Robotic Hand," in *2021 IEEE International Conference on Robotics and Automation (ICRA), IEEE*, May, pp. 1177– 1183, 2021.

[12] Y. Yan, S. Guo, C. Yang, C. Lyu, and L. Zhang, "The PG2 Gripper: an Underactuated Two-fingered Gripper for Planar Manipulation," in *2022 IEEE International Conference on Mechatronics and Automation (ICMA), IEEE*, Aug., pp. 680– 685, 2022.

[13] D. Yoon and K. Kim, "Fully Passive Robotic Finger for Human-Inspired Adaptive Grasping in Environmental Constraints," *IEEE/ASME Transactions on Mechatronics*, vol. 27, no. 5, pp. 3841– 3852, Oct. 2022.

[14] Z. Hu, W. Wan, and K. Harada, "Designing a Mechanical Tool for Robots with Two-Finger Parallel Grippers," *IEEE Robot Autom Lett*, vol. 4, no. 3, pp. 2981– 2988, Jul. 2019.

[15] N. Elangovan, L. Gerez, G. Gao, and M. Liarokapis, "Improving Robotic Manipulation without Sacrificing Grasping Efficiency: A Multi-Modal, Adaptive Gripper with Reconfigurable Finger Bases," *IEEE Access*, vol. 9, pp. 83298– 83308, 2021.

[16] A. Kobayashi, J. Kinugawa, S. Arai, and K. Kosuge, "Design and Development of Compactly Folding Parallel Open-Close Gripper with Wide Stroke," in *2019 IEEE/RSJ International Conference on Intelligent Robots and Systems (IROS)*, IEEE, Nov., pp. 2408– 2414, 2019.

[17] Muslikhin, J. R. Horng, S. Y. Yang, and M. S. Wang, "Object Localization and Depth Estimation for Eye-in-Hand Manipulator Using Mono Camera," *IEEE Access*, vol. 8, pp. 121765– 121779, 2020.

[18] C. Wang, X. Zang, H. Zhang, H. Chen, Z. Lin, and J. Zhao, "Status Identification and Object In-Hand Reorientation Using Force/Torque Sensors," *IEEE Sens J*, vol. 21, no. 18, pp. 20694–20703, Sep. 2021.

[19] J. Li, S. Dong, and E. Adelson, "Slip Detection with Combined Tactile and Visual Information," in *2018 IEEE International Conference on Robotics and Automation (ICRA)*, *IEEE*, May, pp. 7772– 7777, 2018.

[20] E. G. Ribeiro, R. de Queiroz Mendes, and V. Grassi, "Real-time deep learning approach to visual servo control and grasp detection for autonomous robotic manipulation," *Rob Auton Syst*, vol. 139, May 2021.

[21] J. F. Elfferich, D. Dodou, and C. Della Santina, "Soft Robotic Grippers for Crop Handling or Harvesting: A Review," *IEEE Access*, vol. 10, pp. 75428– 75443, 2022.

[22] J. Shintake, V. Cacucciolo, D. Floreano, and H. Shea, "Soft Robotic Grippers," *Advanced Materials*, vol. 30, no. 29. Wiley-VCH Verlag, Jul. 19, 2018.

[23] S. Funabashi, Y. Kage, H. Oka, Y. Sakamoto, and S. Sugano, "Object Picking Using a Two-Fingered Gripper Measuring the Deformation and Slip Detection Based on a 3-Axis Tactile Sensing," in *2021 IEEE/RSJ International Conference on Intelligent Robots and Systems (IROS)*, IEEE, Sep., pp. 3888–3895, 2021.

[24] Z. Kappassov, D. Baimukashev, O. Adiyatov, S. Salakchinov, Y. Massalin and H. A. Varol, "A Series Elastic Tactile Sensing Array for Tactile Exploration of Deformable and Rigid Objects," *2018 IEEE/RSJ International Conference on Intelligent Robots and Systems (IROS)*, Madrid, Spain, pp. 520-525, 2018.

[25] T. P. Tomo *et al.*, "A New Silicone Structure for uSkin—A Soft, Distributed, Digital 3-Axis Skin Sensor and Its Integration on the Humanoid Robot iCub," *IEEE Robot Autom Lett*, vol. 3, no. 3, pp. 2584– 2591, Jul. 2018.

[26] N. F. Lepora, Y. Lin, B. Money-Coomes, and J. Lloyd, "DigiTac: A DIGIT-TacTip Hybrid Tactile Sensor for Comparing Low-Cost High-Resolution Robot Touch," *IEEE Robot Autom Lett*, vol. 7, no. 4, pp. 9382– 9388, Oct. 2022.

[27] H. Khamis, R. Izquierdo Albero, M. Salerno, A. Shah Idil, A. Loizou, and S. J. Redmond, "PapillArray: An incipient slip sensor for dexterous robotic or prosthetic manipulation – design and prototype validation," *Sens Actuators A Phys*, vol. 270, pp. 195– 204, Feb. 2018.

[28] M. Guo, P. Wu, B. Yi, D. Gealy, S. McKinley, and P. Abbeel, "Blue Gripper: A Robust, Low-Cost, and Force-Controlled Robot Hand," in *2019 IEEE 15th International Conference on Automation Science and Engineering (CASE)*, *IEEE*, Aug., pp. 1505– 1510, 2019.

[29] G. Li, P. Xu, S. Qiao, and B. Li, "Stability analysis and optimal enveloping grasp planning of a deployable robotic hand," *Mech Mach Theory*, vol. 158, Apr. 2021.

[30] T. H. G. Megson, "Virtual work and energy methods," in *Aircraft Structures for Engineering Students*, *Elsevier*, pp. 99–130, 2022.